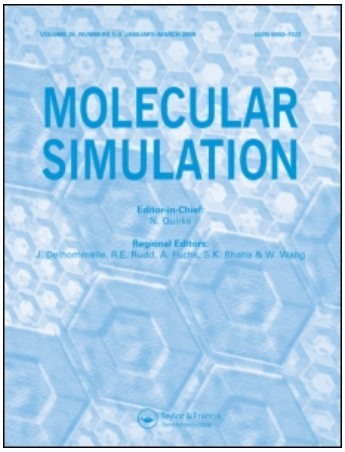

Molecular Simulation
Publication details, including instructions for authors and subscription information:
http://www.informaworld.com/smpp/title~content=t713644482

First-principle study of the native defects in GaAs saturable absorbers

Wenjing Tang[a]; Dechun Li[a]; Shengzhi Zhao[a]; Guiqiu Li[a]; Kejian Yang[a]
[a] School of Information Science and Technology, Shandong University, Jinan, P.R. China

Online publication date: 10 December 2010

To cite this Article Tang, Wenjing , Li, Dechun , Zhao, Shengzhi , Li, Guiqiu and Yang, Kejian(2010) 'First-principle study of the native defects in GaAs saturable absorbers', Molecular Simulation, 36: 14, 1141 — 1147
To link to this Article: DOI: 10.1080/08927022.2010.506514
URL: http://dx.doi.org/10.1080/08927022.2010.506514

Molecular Simulation
Vol. 36, No. 14, December 2010, 1141–1147

Taylor & Francis
Taylor & Francis Group

First-principle study of the native defects in GaAs saturable absorbers

Wenjing Tang, Dechun Li*, Shengzhi Zhao, Guiqiu Li and Kejian Yang

School of Information Science and Technology, Shandong University, Jinan 250100, P.R. China

(*Received 31 March 2010; final version received 27 June 2010*)

The change of atom configuration in GaAs, caused by intrinsic point defects (Ga and As vacancies, Ga and As antisites, Ga and As interstitials), is first calculated by a plane wave pseudo-potential method with the generalised gradient approximation in the frame of density functional theory, and the most stable structure is obtained. Then, the formation energy of each kind of the native defect is calculated, by which the possibilities of the six kinds of point defects to be formed during crystal growth are analysed. The defect energy levels corresponding to each kind of the native point defect and their electron occupancy are analysed from the aspect of density of states. Finally, the elastic constants of GaAs saturable absorbers with native point defects are calculated, and the impacts on the elastic properties brought by native point defects are studied. The values of defect energy levels obtained will be helpful in ascertaining the mechanism of the EL2 deep level in the GaAs saturable absorber, and the analysis of the elastic properties of a GaAs crystal with native point defects will be helpful in guiding the application of the GaAs crystal as a saturable absorber in passively Q-switched lasers.

Keywords: EL2 defect; formation energy; defect energy level; density of states; elastic properties

1. Introduction

Passively Q-switched all-solid-state lasers are of great interest because of their advantages and potential applications in remote sensing, ranging, micromachining and nonlinear wavelength conversion. GaAs saturable absorbers have achieved passive Q-switching for a variety of gain media with the advantages of stable photochemical properties and saturable absorption, good thermal conductivity, no degradation and high damage threshold [1–4]. The band gap of a GaAs crystal is 1.43 eV, which is much higher than the photon energy at 1.06 μm. The main mechanism of passive Q-switching is the effect of deep level (EL2), which is produced by the defects of GaAs raw material [5]. When the laser intensity is small, the single photon absorption caused by photoionisation of the EL2 deep level is the main reason for GaAs passive Q-switching. But the concentration of the EL2 deep-level defect in the perfect GaAs crystal is very low, resulting in a worse saturable absorption and the recovery time that is difficult to control. Therefore, the concentration of the EL2 deep level should be increased by controlling the growth conditions of the GaAs crystal, by which the nonlinear loss, linear loss, recovery time and modulation depth can be controlled.

The EL2 deep level in the middle of the forbidden band of GaAs has been found by researchers as early as 1961, which has been further confirmed by spectral experiments [6]. Up to the present, in addition to much experimental research work, the characteristics and forming reasons of the EL2 deep level have also been extensively studied from the theoretical views [7–10]. However, to our knowledge, there are no definitive conclusions on the microstructure and the forming reasons of the EL2 defect. As for technological and engineering applications, electronic structures and elastic properties are important parameters of solid materials, which can help us to investigate the micromechanism of the EL2 deep level in GaAs. Therefore, it is necessary to know more about the electronic structures and elastic properties of GaAs semiconductor materials.

In addition to a variety of experimental methods, the simulation is also a very effective method for studying the properties of semiconductor materials. In recent years, the first-principle study has emerged to be a powerful tool to predict the electronic structures and elastic properties of defects in semiconductor materials [11,12]. The plane wave pseudo-potential method based on density functional theory (DFT) is a relatively mature method to calculate the electronic structures and properties of the crystal. The pseudo-potential is used instead of the true potential of the particles, the electronic wave functions are expanded by plane wavelet group and the exchange–correlation functions are corrected by the local density approximation (LDA) or generalised gradient approximation (GGA). The electronic structures corresponding to each kind of the native point defect are analysed from the aspect of density of states by the plane wave pseudo-potential method.

In this paper, the defects we want to investigate are intrinsic point defects in the GaAs crystal, namely Ga vacancies (V_{Ga}), As vacancies (V_{As}), Ga interstitials (Ga_i),

*Corresponding author. Email: dechun@sdu.edu.cn

ISSN 0892-7022 print/ISSN 1029-0435 online

DOI: 10.1080/08927022.2010.506514
http://www.informaworld.com

As interstitials (As_i), Ga antisites (Ga_{As}) and As antisites (As_{Ga}) in both the Ga and As sublattices. First, the most stable atomic configuration with different intrinsic point defects should be determined by geometry optimisation. Then, by calculating the formation energy of each kind of intrinsic point defect, the possibilities of the six kinds of defects to be formed during crystal growth and the distribution density of the six kinds of defects in bulk materials under the thermal equilibrium state can be obtained. In addition, the overall density of states is calculated to determine the locations of each defect energy level and the electron occupation. Finally, the elastic constants of the GaAs crystal with different intrinsic point defects were obtained, by which the elastic properties of GaAs saturable absorbers with different intrinsic point defects were studied.

2. Simulation method and model

Cambridge serial total energy package (CASTEP), an *ab initio* pseudo-potential method based on DFT, has been used in this study [13]. GGA with PBE parameterisation is used to describe the exchange–correlation interaction. Ultrasoft pseudo-potentials are used to model the electron–ion interaction. A $2 \times 2 \times 2$ Monkhorst Pack grid of *k*-points is adopted for sampling the Brillouin zone. The point defect structure is represented by a $2 \times 2 \times 2$ face-centred cubic super-cell containing 32 atoms and one point defect is considered at one time. In defect calculations, the experimental values of lattice parameters are used and atomic positions are fully relaxed without any symmetry constraints. The entire system is neutral.

The perfect GaAs crystal is the face-centred cubic structure, each atom and four heterogeneous atoms around form the tetrahedral structure. First, the tetrahedral centre atom is replaced by the space or the antisite atom when a vacancy or an antisite defect is calculated (shown in Figure 1). Then, the atoms' locations of the lowest energy and stress can be obtained by optimising the super-cells. In this paper, the BFGS algorithm [14] is chosen for the geometry optimisation of the super-cells. The energy cut-off for the plane wave basis is chosen as 500 eV for the electronic structure calculation and 300 eV for the elastic constant calculation. Test calculations show that the denser *k*-point grid and higher energy cut-off slightly affect the computational results. The tolerances are set as follows: 5×10^{-6} eV/atom for the total energy when the energy cut-off was 500 eV, 2×10^{-6} eV/atom for the total energy when the energy cut-off was 300 eV, 0.1 eV/nm for the root mean square atomic force and 0.003 for the maximum strain amplitude.

By optimising a variety of geometric structures with different locations of interstitial atoms, we find that interstitial atoms exist in the form of split interstitials which have the lowest energy. Therefore, in this article, the split interstitial models are used for interstitial atoms (shown in Figure 2); other parameters are used as mentioned earlier.

3. Calculation of defect formation energy

The formation energy of a vacancy or an interstitial can be defined [15] as

$$E = E_{N\pm1} - E_N \pm \mu, \tag{1}$$

where $E_{N\pm1}$ represents the total energy of the super-cells with defects; E_N is the total energy of the perfect lattice; μ represents the single-atom chemical potential, which can be obtained from the experimental data or estimated by constructing the cubic cells with appropriate crystal axis length; and the symbol ' $\pm$ ' corresponds to a vacancy or an interstitial defect, respectively. The formation energy of Frenkel defects in the GaAs crystal is the sum of the formation energy of the same kinds of atomic vacancy and interstitial defects, while the formation of Schottky defects requires the energy which can move two kinds of vacancy atoms to the crystal surface to form a new cell:

$$E(\text{Schottky}) = E(V_{As}) + E(V_{Ga}) + E(\text{GaAs})_{\text{unitcell}}, \tag{2}$$

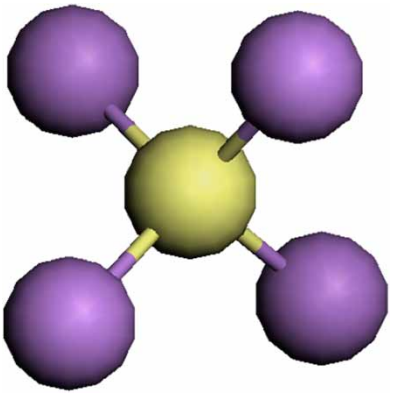

Figure 1. Scheme of the atom configuration in GaAs.

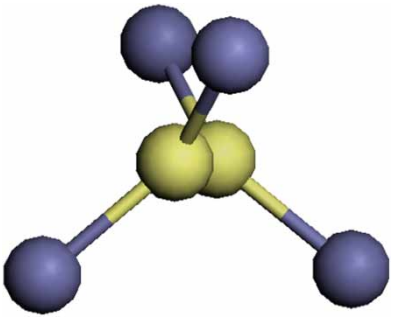

Figure 2. Scheme of the split interstitial configuration.

Table 1. Formation energies (eV) of various point defects in GaAs crystals.

$E(V_{Ga})$	$E(Ga_i)$	$E(V_{As})$	$E(As_i)$	$E(As_{Ga})$	$E(Ga_{As})$	Ga (Frenkel)	As (Frenkel)	Schottky
8.24	−7.82	9.91	−7.67	0.94	4.27	0.42 (0.21)	0.24 (1.12)	15.79 (7.89)

$E(V_{As})$ and $E(V_{Ga})$ is the formation energy of the As vacancy and the Ga vacancy, respectively. $E(GaAs)_{unitcell}$ is the energy of the GaAs single cell.

The formation energy of antisite defects can be calculated, respectively, as follows:

$$E(Ga_{As}) = E_{def} - [E_{per} - E(As) + E(Ga)]$$
$$E(As_{Ga}) = E_{def} - [E_{per} - E(Ga) + E(As)], \quad (3)$$

where E_{per} is the total energy of the perfect GaAs super-cell; E_{def} is the total energy of the GaAs super-cell containing point defects; and $E(As)$ and $E(Ga)$ are the energy of As and Ga atoms, respectively.

The determined formation energy values for intrinsic point defects are summarised in Table 1, and some of them are translated into the formation energies of one point defect in parentheses.

The formation energy we obtained reflects the possibilities of these defects to be formed in the bulk material; the larger the formation energy, the more difficult the information of the defect will be, otherwise it is easy to form. From the calculation results listed in Table 1, it can be seen that the formation energy of Ga Frenkel defects, As Frenkel defects and As antisite defects in the GaAs crystal are smaller, indicating that they are the intrinsic point defects which are relatively easy to form. However, the Schottky defects and Ga antisite defects are more difficult to form, because their formation energies are relatively large; therefore, the Schottky defects and Ga antisite defects in the GaAs crystal are comparatively less.

The calculation results of defect formation energy are all obtained under the condition of the neutral system in this paper; however, for the changes in defect formation energy with the electricity of the defect and the location of the Fermi level, further study by researchers is needed.

4. Electronic structure

The calculated band structures are too complex for analysis as the super-cells used to calculate the defective states are too large. It is more convenient to analyse the electronic structure from the perspective of density of states. The overall distribution of density of states of the GaAs crystal with six kinds of intrinsic point defects is shown in Figure 3. The vertical dotted lines in the figure indicate the position of the Fermi level under the ground state, since the calculation results of the Fermi level's location for each defective state we obtained all demarcated as the location of the zero-point energy, which is not convenient to compare with each other. The energy was re-calibrated in Figure 3 to make the peak of As2s states of a variety of defects located at −5.79 eV consistent with that of the perfect the GaAs. From the perspective of bond formations, the 2s electron of As atoms in the GaAs crystal is not involved. The electron energy should be basically the same with each other because of which the energy levels corresponding to As2s states are deep and little affected by the impurity atoms.

Figure 3 shows the distribution of the total density of states of the perfect GaAs crystal, the width of calculated band gap being about 1.453 eV, which is very close to the experimental value of 1.43 eV. The values of the band gaps' width calculated by the DFT under the LDA and GGA are generally smaller than the experimental values. As the energy of the Ga3d state of the GaAs crystal is overestimated, the interaction between Ga3d and As4p states is increased, resulting in a larger valence bandwidth and a lower band gap. Therefore, by ignoring the effect of the Ga3d state in the calculation, we obtained the values of the band gaps which are much closer to the experimental values.

It can be seen from the distribution of the general density of states of V_{As} and V_{Ga} that the two vacancy defects do not form defect levels in the band gap, but make the valence band and the conduction band wider, resulting in a smaller band gap.

A defect state of the As_{Ga} defect with a certain width is formed between the top of the valence band (VBM) and the bottom of the conduction band (CBM). This is because

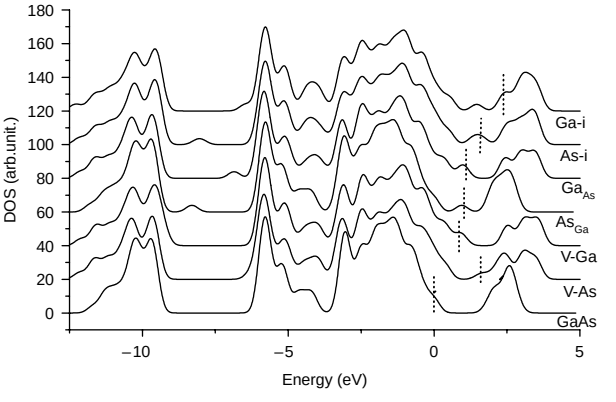

Figure 3. Total density of states for the pure GaAs and the GaAs with native defects (the Fermi-levels are located at the vertical dotted lines).

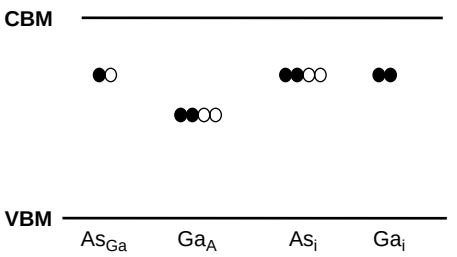

Figure 4. Schemes of energy levels of the native defects in GaAs (solid core dots, occupied by electrons; hollow core dots, not occupied by electrons).

the super-cells used in the calculation are not large enough, the density of defects are too high and the wave functions of adjacent defects overlap, resulting in defect levels extending to the energy band (defect state). In order to facilitate description, we defined the energy centres of defect states as the corresponding defect levels. It can be seen from Figure 3 that the defect level of As_{Ga}, which is located in the middle of the forbidden band (below the CBM at about 0.52 eV), is a deep defect level which is similar to the s-state. This deep level can accommodate two electrons, and the ground state is filled with only one electron.

A deep level of the Ga_{As} defect is also formed in the centre of the forbidden band, which is located below the CBM at about 0.82 eV. It can accommodate four electrons, and the ground state is filled with two electrons.

The deep levels of As_i and Ga_i defects are all formed in the middle of the forbidden band (below the CBM at about 0.5 eV). The defect energy level of As_i can accommodate four electrons, and the ground state is filled with two electrons. The energy level of the Ga_i defect can accommodate two electrons, and the ground state is all occupied.

These results are summarised in Figure 4.

From the analysis of the defect-formation energy, we know that the formation energy of the Ga_{As} defect is relatively large; therefore, there are few Ga_{As} defects in GaAs crystals as they are difficult to produce.

It can be concluded that the formation of the EL2 deep-level defects in GaAs saturable absorbers may be mainly related to As_{Ga}, As_i and Ga_i – three kinds of intrinsic point defects.

5. Analysis of elastic properties

5.1 The lattice constants of the GaAs crystal

As we know, the lattice constant of pure GaAs crystal is a fixed constant. While the existence of intrinsic point defects changes the binding force between atoms, makes the lattice deformation occurred, and at this time the location of atoms is not determined by the crystal symmetry, but the equilibrium position on which the force is zero. Therefore, the lattice constants of GaAs super-cells are changed significantly for the existence of intrinsic point defects.

From Table 2, we can see that the value of the lattice constant of the GaAs super-cell with the As_{Ga} defect is the same as that of the perfect GaAs, but the values of the GaAs super-cells with other intrinsic point defects decrease obviously by about 0.6 nm. Especially, the lattice constants of the GaAs super-cells with the As_i defects in the [100] direction are slightly larger than those of the other two directions.

5.2 The simulation results of the elastic constants

According to Hook's theorem, we can see that the relationships between the stress and strain of the material that has a small deformation can be expressed as: $\sigma_i = c_{ij}\varepsilon_j$ (σ_i represents the components of the stress tensor, ε_j represents the components of the strain tensor, c_{ij} is the elastic constants) [16]. The elastic constants of the GaAs crystal are calculated by computing the components of the stress tensor for a given small applied strain using the CASTEP software. The given strain tensor can be expressed as $\varepsilon = [\varepsilon_{ij}]$, where ε_{ij} $(i, j = 1, 2, 3)$ is a small lattice distortion, and $\varepsilon_{ij} = \varepsilon_{ji}$. Then, the elastic constants C_{ij} can be obtained by using the stress–strain relationship.

To our knowledge, there are only three independent elastic constants of the perfect GaAs crystal: C_{11}, C_{12} and C_{44}, and the relations among them are $C_{11} = C_{22} = C_{33}$, $C_{12} = C_{13} = C_{23}$ and $C_{44} = C_{55} = C_{66}$. However, for the existence of the intrinsic point defects, the symmetry of GaAs crystals is changed significantly, resulting in nine independent elastic constants: C_{11}, C_{22}, C_{33}, C_{12}, C_{13}, C_{23}, C_{44}, C_{55} and C_{66}. The simulation results of the elastic constants are shown in Table 3, which is slightly lower than the experimental data obtained by Dunslan [17]. This is mainly caused by the LDA and GGA methods we used. The same behaviour has been observed for substoichiometric titanium nitrides [18].

From Figure 5, we can see the impact on the elastic constants of GaAs crystals which is made by different intrinsic point defects more intuitively. It is of interest to compare the results obtained from the super-cells with intrinsic point defects with that of the same structure without point defects. The elastic constants of GaAs crystals with As_{Ga} defects are the same as that of the perfect GaAs crystals, while the elastic constants' curve of As_i defects fluctuates most obviously (the values of C_{55} and C_{66} that are not marked in the figure are -166 and -219 GPa, respectively). Moreover, the values of the elastic constants of the GaAs crystal C_{11}, C_{22}, C_{33}, C_{12}, C_{13} and C_{23} become obviously larger than that of the perfect GaAs crystals for the existence of the other four kinds of point defects, and the values of C_{44}, C_{55} and C_{66}

Table 2. Lattice constants (nm) of the GaAs super-cells after geometry optimisation.

Pure GaAs	V_{As}	V_{Ga}	As_i	Ga_i	As_{Ga}	Ga_{As}
$a = b = c = 1.1306$	$a = b = c = 1.0718$	$a = b = c = 1.0733$	$a = 1.0954, b = c = 1.0776$	$a = b = c = 1.0785$	$a = b = c = 1.1306$	$a = b = c = 1.0767$

become smaller slightly. The dependence of the obtained elastic constants on the way that the different strains are applied is attributed to the different modification of the local environment in the GaAs crystal along the different direction [19]. However, the changes of the elastic constants caused by the Ga_i defect are most obvious. Therefore, we can figure out that the mechanical properties of GaAs crystals are mainly affected by the As_i and Ga_i defects.

According to elastic mechanics, we know that the larger the elastic constants of the material, the more difficult the stretching of the material becomes. The elastic constants C_{11}, C_{22}, C_{33}, C_{12}, C_{13} and C_{23} are the ratios of the main stresses and main strains, and C_{44}, C_{55} and C_{66} are the ratios of shear stresses and shear strains. From the simulation results, it can be concluded that the existence of defects makes it easier for the occurrence of tangential deformation in the GaAs crystal; however, the deformation in the principal directions does not occur easily while the hardness of GaAs crystals in the principal directions increases. In addition, from the results of the lattice constants, it can also be found that the elastic constants in the principal directions decrease with increasing lattice constants, which have been found by Wang et al. [20].

5.3 Analysis of the elastic modulus

The simulation results also give the values of Young's modulus E, bulk modulus B, shear modulus G, Poisson's ratio ν, compressibility K and Lame lambda of GaAs crystals.

Figure 6 shows the values of Young's modulus E_X, E_Y and E_Z of the GaAs crystal with defects in the direction of [100], [010] and [001], as well as the simulation results of the bulk modulus, shear modulus and Lame lambda.

The Voigt–Reuss–Hill approximate models are used in the CASTEP software to calculate the bulk modulus, shear modulus and Lame lambda. The simulation results of Voigt and Reuss models are the upper and lower limits of the elastic modulus, respectively. Hill model calculates the elastic modulus by taking arithmetic means of the extremes obtained by the Voigt and Reuss models [21]. In Figure 6, B_H, G_H and $Lame_H$ represent the bulk modulus, shear modulus and Lame lambda obtained by the Hill model, respectively.

As we know, Young's modulus of the perfect GaAs crystal is a constant, while the existence of intrinsic point defects makes the values of Young's modulus vary with different directions we have mentioned. It can be seen from Figure 6 that the differences in Young's modulus in three directions caused by the Ga_{As} and As_i point defects are larger, especially, for the As_i defects, E_Y is much larger than E_X and E_Z. Also, the values of Young's modulus of the GaAs crystals with defects are slightly smaller than that of

Table 3. Values of the elastic constants (GPa) for pure GaAs and GaAs with native defects.

	C_{11}	C_{22}	C_{33}	C_{12}	C_{13}	C_{23}	C_{44}	C_{55}	C_{66}
Pure GaAs	98.47	98.48	98.51	15.25	15.27	15.27	57.89	57.90	57.90
V_{As}	132.84	131.35	131.62	57.14	57.18	56.93	59.63	55.73	59.84
As_{Ga}	98.47	98.48	98.51	15.25	15.27	15.27	57.89	57.90	57.90
As_i	145.59	65.23	70.05	43.55	60.07	65.23	73.59	−166.04	−219.92
V_{Ga}	125.92	125.84	126.56	61.32	61.54	61.58	52.80	52.69	52.76
Ga_{As}	130.99	127.43	125.67	70.13	70.57	71.37	50.87	48.70	46.11
Ga_i	124.94	124.97	124.96	72.62	72.62	72.59	41.19	40.74	40.72

the perfect GaAs crystals. In addition, it can be found from Figure 6 that the existence of defects (especially the Ga_{As} and As_i defects) increases the bulk modulus B_H and the Lame lambda $Lame_H$ and decreases the shear modulus G_H.

The existence of intrinsic point defects in GaAs crystals reduces the ability to resist the shear deformation,

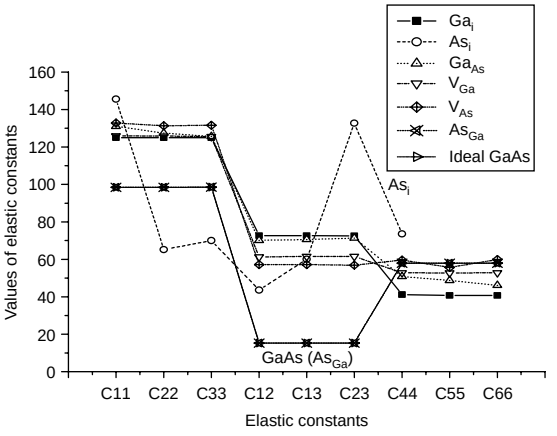

Figure 5. Analysis of elastic constants for pure GaAs and GaAs with native defects.

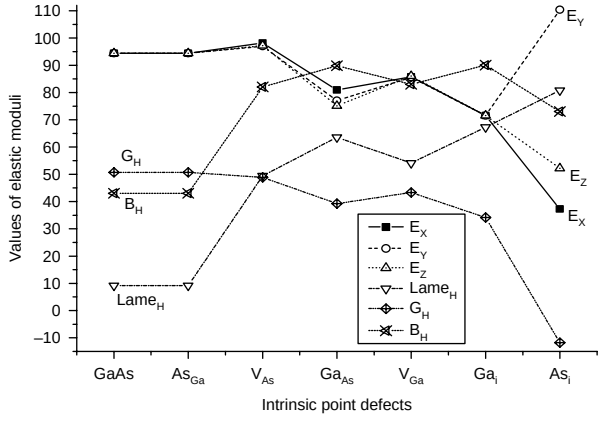

Figure 6. Analysis of Young's moduli, elastic moduli B and G, and Lame constant for pure GaAs and GaAs with native defects.

but enhances the bonding strength of the GaAs crystals, and the atoms are integrated with each other even more closer. Thus, the bulk modulus B_H slightly increased, which is consistent with the conclusion of Table 3.

This phenomenon can also be understood by introducing an experience criteria proposed by Pugh [22], which is usually utilised to evaluate the ductility or the brittleness of materials by calculating the ratios of the shear modulus G and the bulk modulus B. By considering that the shear modulus is associated with the resistance to plastic deformation and the bulk modulus is associated with the resistance to fracture, Pugh brought up that the material is ductile if $G/B < 0.5$, otherwise the material is brittle. From our calculations, we know that if the value of G/B of the pure GaAs is larger than 0.5, then it can be figured out that the pure GaAs is a brittle material, which is not easy to extend or break. Furthermore, the value of G/B of GaAs crystals with defects is smaller than that of the perfect GaAs, indicating that the defects in GaAs crystals reduce the brittleness of the crystal and enhance the ability to resist fission.

Table 4 shows the simulation results of Poisson's ratio ν and compressibility K of GaAs crystals with different intrinsic point defects. Poisson's ratio ν can show the stability of a crystal against shear and no volume change during uniaxial deformation if ν is 0.5. Poisson's ratio ν can also be considered as a parameter to measure the brittle degrees of the materials. Poisson's ratios of ductile materials are usually equal to 1/3, which is larger than the values of brittle materials. The values of Poisson's ratios in Table 4 can further prove the conclusions we have obtained above.

Finally, from the analysis of the elastic modulus of GaAs crystals, it can be concluded that the GaAs crystal with the intrinsic point defects has a certain ductility,

Table 4. Simulation results of Poisson's ratios and compression ratios of the GaAs crystal.

	GaAs	V_{As}	As_{Ga}	As_i	V_{Ga}	Ga_{As}	Ga_i
ν	0.13	0.3	0.13	0.28	0.33	0.33	0.37
K	0.023	0.012	0.023	0.016	0.012	0.011	0.011

compared to the perfect GaAs crystal, having the ability to resist fission.

6. Conclusion

The six kinds of intrinsic point defects in GaAs saturable absorbers are first studied by a plane wave pseudopotential method with the GGA in the frame of DFT. The defect formation energy and the overall density of states of intrinsic point defects in GaAs saturable absorbers are calculated, as well as the elastic constants of the perfect GaAs and the GaAs with intrinsic point defects. From the analysis of the defect formation energy and electronic structures of the intrinsic point defects, it can be determined that the EL2 deep-level defects in GaAs saturable absorbers mainly relate to As_{Ga}, As_i and Ga_i, three kinds of intrinsic point defects. Also, the simulation results of the elastic constants demonstrate that the elastic properties of GaAs saturable absorbers are also mainly affected by the Ga_{As}, As_i and Ga_i defects, resulting in nine independent elastic constants: C_{11}, C_{22}, C_{33}, C_{12}, C_{13}, C_{23}, C_{44}, C_{55} and C_{66}.

In short, it can be concluded from our calculation that the characteristics of GaAs saturable absorbers are mainly affected by Ga_{As}, As_i and Ga_i, three kinds of intrinsic point defects, the other three kinds of point defects have little effect on GaAs saturable absorbers.

The results of the present work could be employed for further work on the simulations of multiscale materials [23,24]. Further studies are in progress to examine the presence of other defects as well as the type of atomic interactions on the mechanical properties of nanomaterials.

Acknowledgements

This work was partially supported by the Natural Science Foundation of Shandong Province (Y2007G17) and the National Science Foundation of China (60876056) and the China Postdoctoral Science Foundation-funded project (20090461210).

References

[1] Z. Zhang, L. Qian, and D. Fan, *Gallium arsenide: A new material to accomplish passively mode-locked Nd:YAG laser*, Appl. Phys. Lett. 60 (1992), pp. 419–421.

[2] T.T. Kajava and A.L. Gaeta, *Q-switching of a laser-pumped Nd:YAG laser with GaAs*, Opt. Lett. 21 (1996), pp. 1244–1246.

[3] J. Gu, F. Zhou, and T. Kah, *Q-switching of a diode-pumped Nd:YVO_4 laser with GaAs nonlinear output coupler*, Opt. Lasers Eng. 35 (2001), pp. 299–307.

[4] J. Gu, F. Zhou, and W. Xie, *Passive Q-switching of a diode pumped Nd:YAG with GaAs output coupler*, Opt. Commun. 165 (1999), pp. 245–249.

[5] A.L. Smirl, G.C. Valley, and K.M. Bohnert, *Picosecond photorefractive and free-carrier transient energy transfer in GaAs at 1 μm*, IEEE J. Quantum Electron. 24 (1988), pp. 289–303.

[6] R. Williams, *Determination of deep centers in conducting gallium arsenide*, J. Appl. Phys. 37 (1966), p. 3411.

[7] M. Kaminska, M. Skowronskii, and W. Kuszko, *Identification of the 0.82-eV electron trap, EL2 in GaAs, as an isolated antisite arsenic defect*, Phys. Rev. Lett. 55 (1985), pp. 2204–2207.

[8] M. Levinson and J.A. Kafalas, *Site symmetry of the EL2 center in GaAs*, Phys. Rev. B 35 (1987), pp. 9383–9386.

[9] J.F. Wager and J.A. Van Vechten, *Atomic model for the EL2 defect in GaAs*, Phys. Rev. B 35 (1987), pp. 2330–2339.

[10] H.J. Von Bardeleben, D. Stievenard, D. Deresmes, and A. Huber, *Identification of a defect in a semiconductor: EL2 in GaAs*, Phys. Rev. B 34 (1986), pp. 7192–7202.

[11] S. Sanvito and N.A. Hill, *First principles study of intrinsic defects in (Ga,Mn)As*, J. Magn. Magn. Mater. 242–245 (2002), pp. 441–446.

[12] T.Y. Tan, *Point defects and diffusion mechanisms pertinent to the Ga sublattice of GaAs*, Mater. Chem. Phys. 40 (1995), pp. 245–252.

[13] M.D. Segall, P.J.D. Lindan, M.J. Probert, and C.J. Pickard, *First-principles simulation: Ideas, illustrations and the CASTEP code*, J. Phys.: Condens. Matter. 14 (2002), pp. 2717–2744.

[14] Q. Yao, H. Xing, and L. Meng, *Theoretical calculation of elastic properties of T_iB_2 and T_iB*, Chin. J. Nonferr. Metals 17 (2007), pp. 1297–1301.

[15] J.E. Davis, R.S. Hughes, and H.W.H. Lee, *Ultraviolet-induced transient absorption in potassium dihydrogen phosphate and its influence on frequency conversion*, Chem. Phys. Lett. 207 (1993), pp. 540–543.

[16] M.J. Mehl, *Pressure dependence of the elastic moduli in aluminum-rich Al–Li compounds*, Phys. Rev. B 47(5) (1993), pp. 2493–2500.

[17] D. Dunslan, in *Properties of GaAs*, M. Brozel and G. Stillmann, eds., Inspec, London, 1996.

[18] M. Guemmaz, A. Mosser, R. Ahuja, and J.C. Parlebas, *Theoretical and experimental investigations on elastic properties of sub-stoichiometric titanium nitrides: Influence of lattice vacancies*, Int. J. Inorg. Mater. 3 (2001), pp. 1319–1321.

[19] T.E. Karakasidis and C.A. Charitidis, *Vacancy effect on the elastic constants of layer-structured nanomaterials*, Theor. Appl. Fract. Mech. 51(3) (2009), pp. 195–201.

[20] Y. Wang, K. Duncan, and E.D. Wachsman, *The effect of oxygen vacancy concentration on the elastic modulus of fluorite-structured oxides*, Solid State Ionics 178 (2007), pp. 53–58.

[21] O.L. Aaderson, *A simplified method for calculating the Debye temperature from elastic constants*, J. Phys. Chem. Solids 24 (1963), pp. 909–917.

[22] S.F. Pugh, *Relations between the elastic moduli and the plastic properties of polycrystalline pure metals*, Philos. Mag. 45 (1954), pp. 823–843.

[23] T.E. Karakasidis and C.A. Charitidis, *Multiscale modeling in nanomaterials science*, Mater. Sci. Eng. C 27 (2007), pp. 1082–1089.

[24] Q.X. Wang, T.Y. Ng, H. Li, and K.Y. Lam, *Multiscale simulation of coupled length-scales via meshless method and molecular dynamics*, Mech. Adv. Mater. Struct. 16 (2009), pp. 1–11.